



## Bacterial detection using bacteriophages and gold nanorods by following time-dependent changes in Raman spectral signals

Farzaneh Moghtader<sup>a,b</sup>, Aysel Tomak<sup>c</sup>, Hadi M. Zareie<sup>d</sup> and Erhan Piskin<sup>b,e</sup>

<sup>a</sup>Division of Nanotechnology and Nanomedicine, The Institute for Graduate School of Science and Engineering, Hacettepe University, Ankara, Turkey; <sup>b</sup>NanoBMT: Cyberpark-Bilkent/KOSGEB-Başkent University-Tekmer, Ankara, Turkey; <sup>c</sup>Department of Material Science and Engineering Department, Izmir Institute of Technology, Izmir, Turkey; <sup>d</sup>School of Mathematical and Physical Science (Physics), University of Technology Sydney, Sydney, Australia; <sup>e</sup>Department of Chemical Engineering, Hacettepe University, Ankara, Turkey

### ABSTRACT

This study attempts to develop bacterial detection strategies using bacteriophages and gold nanorods (GNRs) by Raman spectral analysis. *Escherichia coli* was selected as the target and its specific phage was used as the bioprobe. Target bacteria and phages were propagated/purified by traditional techniques. GNRs were synthesized by using hexadecyltrimethyl ammonium bromide (CTAB) as stabilizer. A two-step detection strategy was applied: Firstly, the target bacteria were interacted with GNRs in suspensions, and then they were dropped onto silica substrates for detection. It was possible to obtain clear surface-enhanced Raman spectroscopy (SERS) peaks of the target bacteria, even without using phages. In the second step, the phage nanoemulsions were dropped onto the bacterial–GNRs complexes on those surfaces and time-dependent changes in the Raman spectra were monitored at different time intervals upto 40 min. These results demonstrated that how one can apply phages with plasmonic nanoparticles for detection of pathogenic bacteria very effectively in a quite simple test.

### ARTICLE HISTORY

Received 10 February 2018  
Revised 10 March 2018  
Accepted 11 March 2018

### KEYWORDS

Bacterial detection;  
*Escherichia coli*;  
gold nanorods;  
T4-bacteriophages; Raman  
spectral analysis;  
time dependent

### Introduction

Food and water borne diseases are among the most serious and costly public health concerns worldwide. They are still one of the major causes of morbidity, in spite of modern technologies and safety concerns. Food and water are the most important resources for humans, but unfortunately for microorganisms as well. Transfer of the pathogenic bacteria via contaminated food/water consumption is a common among daily event and is the major route for serious infections [1,2]. Therefore, it is obvious that bacterial contaminations in food/water must be detected/monitored very effectively and efficiently in all stages of production, processing, transportation and consumption. Development of fast, accurate and sensitive detection and monitoring of pathogens, which should be miniaturized/portable automated therefore cost effective, is a very important challenge.

There are a number of pathogenic bacteria that may cause severe infections including *Escherichia coli* (*E. coli*) which is – a gram negative bacteria – a rather common family – responsible bacterial contaminations in food and water and some strains are highly pathogenic (such as *E. coli* O157:H7 and O104:H4) causing gastrointestinal diseases, serious outbreaks but even death [3–7]. Therefore, *E. coli* has globally become one of the main target bacteria to be detected and cured. A rather safe strain *E. coli* K12 was selected/used in the present study as the target for demonstration of the detection protocol proposed here.

Current pathogen detection methods include: (i) microbiological techniques (conventional culturing); (ii) nucleic-acid based (e.g. PCR and DNA hybridization using oligonucleotides as bio-recognition elements – “bioprobes”) and (iii) immunological (e.g. ELISA – with specific antibodies as bioprobes) [8–13]. Using bacteriophages as bioprobes alternative to antibodies and nucleic acids for bacterial detection is a very unique approach and that have been proposed rather recently [14–17]. Bacteriophages are viruses, which only infect bacteria, with excellent host selectivity. Bacteriophages are not only the most abundant biological entities but also the most diverse ones. They may be very specific even at serotype levels, could be easily propagated and therefore are quite in expensive and additionally they have long-shelf life. As nicely reviewed recently by Singh et al. bacteriophages have been used for specific detection of target bacteria by using different bio-sensing platforms, which are mainly treated in the following two categories. (i) using labels (including fluorescent, luminescent, enzymes, electrochemically active labels, etc.), (ii) label-free systems (QCM, SPR, Ellipsometer, Raman and Mass spectrometers, etc.). Almost all of technologies mentioned above have been applied for detection of pathogens by using bacteriophages with different extent and success. The challenging objective is to develop enhanced detection technologies with high levels of reliability, sensitivity, and selectivity with short assay times.

Surface-enhanced Raman spectroscopy (SERS) is one of the most popular label free techniques for detection several

biological molecules/entities including several bacteria with high sensitivity/detection limits [16,17]. Several metallic nanostructures exhibiting localized plasmon effects are used for enhancing the Raman signals which depends on several factors including size, shape, agglomeration and/or surface oriented/pattern structures, and so on. In recent years due to the "size and shape-dependent" properties metallic, especially gold and silver nanoparticles have been extensively studied in wide variety of applications, such as photonics, information storage, electronic and optical detection systems, therapeutics, diagnostics, photovoltaics, and catalysis. Especially the followings make them excellent materials also for bio-based applications: (i) easy to produce in many different shapes (nanospheres, nanorods, nanocages, nanocubes, etc.) and sizes even down to few nm; (ii) excellent and variable optical (plasmonic) properties; (iii) small sizes means high surface areas; (iv) easy surface modification/functionalization for bioprobe immobilization, etc. Gold nanorods (GNRs) are rod-shape nanoparticles, which could easily produced with different aspect ratios (dimensions) – means different plasmonic properties [18]. Their unique optical and physical properties have allowed using them for development of bio-sensing platforms [19–25]. Therefore, we have also selected, synthesized and utilized GNRs as surface enhancer in our SERS studies reported in this article.

Raman spectra for many rather small molecules/biomolecules are very unique and as a result are commonly called "fingerprints". However, bacteria are quite big entities and maybe considered as a big pool composed of a huge number/variety of biological molecules – some of them with similar compositions (such as amino acids/proteins). Consequently, it is almost impossible to collect a characteristic set of spectra of different bacteria that would allow us to identify the type those complex structures – which is a very challenging topic of research.

Holt and Cotton [26] were the pioneers to apply SERS for identification of microorganisms. Then usually silver nanoparticles have been studied as surface enhancer in Raman spectroscopy in the detection and identification of bacteria (e.g. *E. coli*) by several groups [27–32]. In these studies, unmodified nanoparticles are interacted with the target bacteria in suspensions, dropped onto a platform and then Raman spectra are obtained which is also the main/simple protocol that was applied in this study. It was demonstrated that silver nanoparticles are preferentially accumulated to the Flavin sites, and therefore those bands on the Raman spectra are considered as target points for specificity on the bacterial cells walls. However, there are noticeable differences in the Raman spectra reported by different groups for the same (similar) bacteria which is usually *E. coli* but also similarities in the peak positions and also intensities of the SERS spectra obtained by different groups. These differences may be due to different methods of sample preparation and measurement and possible conformational changes of the cellular proteins when the cells are immobilized on a dry glass surface, and also colloid reproducibility, particle size and aggregation, and their relative number to the target bacteria within the medium may also influence the magnitude of enhancement therefore the intensities. Not only silver but

also gold nanoparticles were used. For instance, Lan et al have investigated detection of *E. coli* and *Salmonella typhimurium* (*S. typhimurium*) by using gold nanoparticles by Raman scattering [33]. It was stated that there are strict differences in the peak position and relative strength. In order to distinguish the differences in various species they have classified all of spectra by principal component analysis (PCA) and hierarchical cluster analysis (HCA) for bacterial identification [33,34].

It should be noted that most of the studies based on SERS based detection of *E. coli* bacteria using bare nanoparticles are based on spectral differentiation at high concentrations and are susceptible to interferences from the culture medium [35]. These are important points and limitations should be considered carefully.

Another important step to reach selective and more precision bacterial detection/identification of target bacteria with SERS was to use targeting molecules on the nanoparticle enhancers which are usually antibodies against bacterial cell surface antigenic groups. Some interesting studies on this line are as follows: Naja et al. have studied detection of *E. coli* by SERS using silver nanoparticles modified with antibodies in which immobilization protocol was somewhat different – they have used protein – as a linker – which was assigned on the SERS spectra for better characterization [36]. Characteristic peaks were assigned clearly similar to the related literature [27,28,30,32,37–40]. It has been proposed that the SERS enhancement mechanism depends upon the metal surface proximity, 8nm was considered as the optimum distance between the bacterium and the nanoparticle surface which was an interesting note.

Guyen et al. [41] have combined immunomagnetic separation (IMS) and SERS to detect *E. coli* in which gold-coated magnetic spherical nanoparticles carrying anti-*E. coli* antibodies were prepared and used for IMS. GNRs carrying Raman labels have (5,5-dithiobis-2-nitrobenzoic acid – DTNB) were used for detection of the target bacteria with SERS. The fingerprints of DTNB-labels on the GNRs were followed for detection – not the specific peaks of *E. coli*. Therefore, they did not attempt to assign SERS peaks of the target bacteria. The correlation between the concentration of bacteria and SERS signal was found to be linear within the range of  $10^1$ – $10^4$  cfu/mL which was quite good alternative approach for specific detection of the target bacteria. Tamer et al. [42] have studied gold coated magnetite nanoparticles further modified with self-assembling molecules against glycoside moieties on the surface of the target bacteria (i.e. *E. coli*). They were able to demonstrate specific targeting and enhancement in the Raman signals in several specific peaks, but not assigned properly.

Recently, Srivastava et al. [7] have reported a different and successful methodology for the detection of *E. coli* – a nanobiosensor chip, utilizing nanosculptured thin films of silver as enhancer for the Raman probe reader. They have immobilized T4 bacteriophages onto the surface of the chip for the specific capture of target *E. coli* bacteria. Results showed that the present sensor performs a fast, accurate and stable detection of *E. coli* with ultra-small concentrations of bacteria down to

the level of a single bacterium in 10  $\mu\text{L}$  volume of the sample which was a quite successful approach.

This study is designed to detect target bacteria (which is *E. coli* K12) using the specific phage (T4 here) as bioprobes and GNRs with well-defined plasmonic properties (for surface enhancement) without need of the peak assignments on the SERS spectra neither for the bacteria nor its phages – but just following the changes in the intensity of some specific peaks with time – a rather simple and novel approach – which is the main and attractive rationale of the present study.

## Experimental

### Propagation of bacteria and bacteriophages

The following bacterial culture media and buffers were prepared freshly and used. All the respective reagents were purchased from Sigma-Aldrich (Munich, Germany). About 25 g of the Luria Bertani (LB) powder was dissolved in 1 L of distilled water to obtain the LB medium which was prepared by adding 6 g of agar into 400 ml of LB media to prepare the LB-agar medium. The SM buffer was prepared by dissolving 5.8 g of NaCl, 2 g of  $\text{MgSO}_4 \cdot 7\text{H}_2\text{O}$ , 50 ml of 1 M Tris-hydrochloride (pH 7.5) and 1 ml of 10% (w/v) gelatine in 1 L of distilled water. Tryptic soy broth (TSB) was made by dissolving 15 g of tryptone, 5 g of soytone and 5 g of NaCl in 1 L of distilled water. The LB medium and buffers were autoclaved prior to use.

The target bacteria, *Escherichia coli* K12 was propagated by a similar protocol that was widely used including our previous studies [25,43–45] which is as follows: The bacteria were first cultured in the sterile LB medium (25 g LB powder in 1 L of distilled water) at 37 °C in a rotary shaker (200 rpm) until to reach the exponential growth phase (about OD 600 nm) – which was followed spectrophotometrically. These bacterial cultures were centrifuged (at 6000 rpm for 5 min) and the pellets precipitated were washed few times and re-suspended in the sterile PBS buffer with a pH of 7.2 (composed of 140 mM NaCl, 2.7 mM KCl, 0.1 mM  $\text{Na}_2\text{HPO}_4$  and 1.8 mM  $\text{KH}_2\text{PO}_4$ ). This suspension was diluted to reach the desired/different concentrations and then plated in the LB agar (prepared by adding 6 g of granulated agar to 400 ml of LB media) and the total bacterial (viable) counts (colour forming units, CFU) were estimated.

T4 phages were amplified using the bacterial suspension prepared in the previous step. In a typical protocol *E. coli* K12 and T4 taken from the stock suspensions – 100  $\mu\text{L}$  of each with concentrations of  $10^8$  CFU/mL and  $10^8$  PFU/mL, respectively. They were mixed in a test tube by using a vortex, incubated at room temperature for 15 min and added to a 20 ml tube containing the LB medium, which was then incubated for 6 h at 37 °C in a shaking incubator (200 rpm). In the final step, chloroform was added – 10% (v/v) – which was kept at 4 °C for about 20 min. For purification, the medium was first ultra-filtered through a sterile 0.22  $\mu\text{m}$  filter to remove any remaining bacteria and then centrifuged at 4 °C (12,000g). The precipitated/purified phages were then re-suspended in the sterile PBS buffer. In order to obtain the phage concentration – as plaque forming unit per ml (PFU/mL) – the

following protocol was applied. The phage suspension prepared in the previous step was diluted to obtain a series of phage suspensions with different phage contents. About 100  $\mu\text{L}$  from each of those phage suspensions and 400  $\mu\text{L}$  of the *E. coli* suspension were mixed, added to the semi-liquid LB-agar (agar 7.5 g/L) and incubated at 37 °C for 24 h. The titration was performed by direct counting of lysis plaques. The phage stock produced were kept in the SM buffer.

The activity and specificity of T4 phages were demonstrated in typical bacterial culture tests. Plates containing the target bacteria *E. coli* on agar broth were prepared. The T4 phages were put on the plates, which were then incubated at 37 °C overnight. Note that the *E. coli* lawn plates were originally turbid, but transparent zones were formed around the phage inserted areas which shows the activity of the T4 phages propagated in the previous steps.

Note that fresh bacterial cultures were prepared from the stock solutions for each new SERS test group – in each day by incubating overnight at 37 °C. After incubation, broth of each culture was transferred to 15 ml sterile centrifuge tubes, and centrifuged at room temperature at 5000 rpm for 10 min (Wisepin; Daihan Scientific, Sinpyoungsukhwaro, Korea). Bacterial pellets were washed by suspending in 10 ml of sterile deionized water and centrifuging for three times. Phages were taken from stocks which were purified previously and stored at 4 °C. The bacteria and phages with concentrations of  $10^8$  PFU/mL and  $10^8$  CFU/mL, respectively were used in the SERS studies demonstrated here.

### Gold nanorods

Hexadecyltrimethylammonium bromide (CTAB), tetrachloroauric (III) acid ( $\text{HAuCl}_4$ ) and sodium borohydride ( $\text{NaBH}_4$ ), and others were bought from Sigma-Aldrich (Munich, Germany) with high purity ( $\geq 99\%$ ) and used as received. DI water (18.2 M $\Omega$ /cm) treated through reverse osmosis (Thermo Scientific, Waltham, MA, USA) was used for preparing all solutions.

The GNRs were produced by a rather classical two-step process as also described in the related literature including ours, which is briefly as follows [25,46–49]. In the first step, in order to synthesize gold spherical nanoparticles, a 7.5 ml–100 mM aqueous solution of CTAB was sonicated for 20 min at 40 °C in a water bath. A 250  $\mu\text{L}$ –10 mM  $\text{HAuCl}_4 \cdot 3\text{H}_2\text{O}$  aqueous solution was added with continuous stirring under nitrogen atmosphere to the CTAB solution. Then, 600  $\mu\text{L}$ –10 mM ice-cold aqueous solution of  $\text{NaBH}_4$  was added under vigorous stirring in 1 min. The CTAB-capped nanospheres formed were used as seeds within 2–5 h for preparation of the GNRs in the next step. A 40 ml of a growth solution consists of CTAB (100 mM) and  $\text{HAuCl}_4 \cdot 3\text{H}_2\text{O}$  (10 mM) was prepared which was dark-yellow. A 250  $\mu\text{L}$ –10 mM  $\text{AgNO}_3$ , aqueous solution and then a 270  $\mu\text{L}$ –100 mM ascorbic acid – a mild reducing agent – (Sigma-Aldrich, St. Louis, MO, USA) were added to the growth solution flask, which resulted a colourless solution. Then, 210  $\mu\text{L}$  of the CTAB-capped seed solution that was produced in the previous step was added to that flask, and the mixture was gently mixed. After 3 h at 24 °C, the colour of the mixture turned into a dark-blue solution with a brownish opalescence, which was an indication of

formation of GNRs. In order to remove most of the surfactants (CTAB) used in the preparation of the GNRs, the nanoemulsions were centrifuged at 13,500g (Wisepin; Daihan Scientific, Sinpyoungsukhwaro, Korea) and re-suspended in DI water (18.2 M $\Omega$ /cm) treated through reverse osmosis (Thermo Scientific, Waltham, MA, USA) and sonicated for about one hour (Wiseclean; Wised Laboratory Instruments, PRC). This cleaning protocol was repeated at least three times.

### Characterization

The scanning electron microscopy (SEM) micrographs of the GNRs, target bacteria and its respective phages, on the substrate ("silicon wafer") surfaces were taken using a Philips Ultra Plus High Resolution FESEM equipped with an in-lens secondary-electron detector at operating range 2–20 keV depending on sample charging (Philips, FEI, Eindhoven, The Netherlands). The suspensions were dropped onto the silica substrate, dried at room temperature and then images were obtained.

Absorption peaks of the nanoemulsions were obtained by using an Ocean Optics USB2000 + VIS/NIR spectrometer (350–1100 nm) (Nanodev Ltd., Ankara, Turkey). All absorbance spectra were collected using quartz cuvettes.

### Detection with Raman spectral analysis

The Raman spectrometer XploRA (Horiba, Longjumeau, France) used in this study is equipped with an Olympus BX41 transmission and reflection illumination microscope (Olympus, Rungis, France). For imaging the 785 laser was used. Raman signals were recorded in a spectral range of 450–3000 cm<sup>-1</sup>, at 50 mW power, in combination with different objectives 10 $\times$ , 40 $\times$  and 100 $\times$  objective magnification (NA=0.25) of the microscope for focus and collection of Raman-scattered light. For each sample, the Raman spectra were taken minimum five different locations on the SERS platform – repeated more than 15 times and averaged to

demonstrate the spectra. Each spectrum was normalized using the Labspec software.

One of the main objectives of this study is to obtain SERS data of the target bacteria using GNRs *without using any SERS substrate*. To demonstrate this approach – "for the proof of the concept" – the GNRs were added to the target bacteria suspensions, incubated at room temperature for 10–30 min, then they were dropped onto the silicon wafers, dried and confocal microscopy (attached to the Raman Spectrometer) images were taken and SERS data were collected. Note that we focused onto individual bacteria and took the SERS image – means our data was corresponding even *single bacterial* detection.

## Results and discussion

### GNRs produced

Gold nanorods were synthesized by a two-step process described in the previous section. A representative UV–vis absorption spectrum of the GNRs synthesized/used in this study is given in Figure 1(A). As seen here two peaks at 510 nm and 670 nm are due to the radius and length, respectively. It should be noted that both the position and intensity of the peaks are representative properties of those GNRs produced. The SEM micrograph given in Figure 1(B) shows that the GNRs produced here are quite homogeneous in size and shape – there are only few nanospheres (seed particles) left from the first step – which demonstrates the success of the synthesis protocol applied here. The average sizes of GNRs that we have used in the later parts of this study were 10 $\pm$ 2 nm (diameter) and 30 $\pm$ 5 nm (length) and according to SEM analysis – estimated with a classical software (Adobe Photoshop CS6).

### SEM images

Representative SEM images of the components used in this study which are taken on the basic substrate platform –

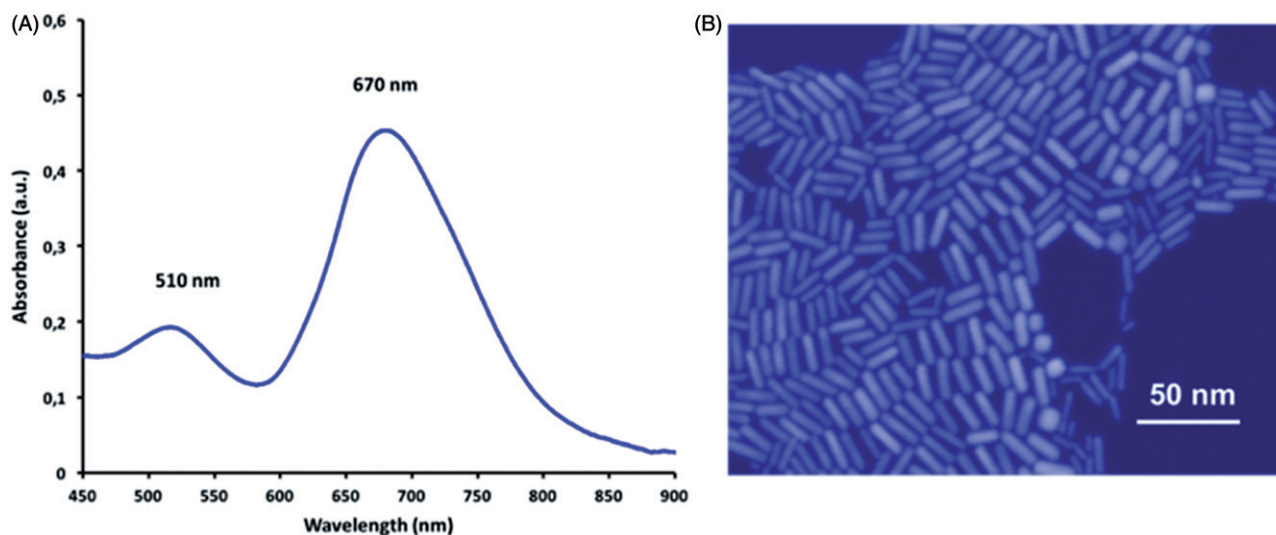


**Figure 1.** The GNRs synthesized of in this study. (A) A representative UV–vis absorption spectrum; and (B) a typical SEM image of the GNRs. A scanning probe image processing was applied.



“silicon wafers” – are given in Figure 2. It should be noticed that the magnifications are different in those SEM images as seen on the scale bars. The GNRs are clearly observable which are with quite narrow size distribution (Figure 2(A)) – as also presented in the previous section (Figure 1). However, it was difficult to obtain the SEM images of the phages on the substrate surfaces – since we have not applied any pre-fixing protocol – just dropped the phage emulsions on the silica platform. Therefore, phages look different in size – there are small and large ones – these should be due to some aggregations and some possible destructions due to high energy applied to obtain the SEM images. Therefore, we have not attempted to describe the average size of the T4 phages by using those images. The images of *E. coli* are typical, as also demonstrated in the related literature (Figure 2(C)). They are in cylindrical shape and kept their original form during SEM imaging. Figure 2(D) shows a representative image of *E. coli* after they were interacted with their specific T4 phages in early phase of phage invasion. As seen here some of the bacteria were already invaded (destroyed) by T4 phages. Representative SEM images of the target bacteria, *E. coli* after interactions with the GNRs in suspension (then dropped on the platform surfaces) are given in Figure 2(E). As seen here positively charged GNRs were accumulated on the negatively charged bacterial surfaces quite heavily and evenly, which allowed clear detection of the target bacteria without using any SERS substrate – on the simple silicon wafer surface as also discussed below. Three main components of the system, i.e. *E. coli* + GNRs attached to the bacteria + T4 phages accumulated also on their target bacteria are shown together in the same figure (Figure 2(F)) which was taken at very early stage – no bacterial destruction yet – only GNRs and T4 phages were accumulated on *E. coli* – the target bacteria).

The phages on their target surfaces look quite healthy and kept their shapes intact comparing to Figure 2(B).

### Raman spectral analysis

Before collecting the Raman signals, we have first observed the surfaces with the Olympus BX41 transmission and reflection illumination microscope attached to the Raman spectrometer that we have used in this study. In order to demonstrate the power of the microscope, several images were taken at different steps of the SERS analysis. Figure 3 gives representative images: (A) *E. coli* K12 on the substrate surfaces; (B) after additions of the nanoemulsions of GNRs onto those surface – notice that the GNRs are accumulated on the bacteria and create a shining red brown colour; and (C) about 30–40 min after addition of the T4 phages onto the previous surface in which the bacteria have already totally destroyed by the T4 phages and images “look like lubricated with oil” were observed. Note that this was not the protocol that we have used in the SERS analysis – which is described below – however it demonstrates what is happening on the surfaces and exhibits of the power of our Raman system.

One of the main objectives of this study is to obtain SERS data of the target bacteria using GNRs *without using any SERS substrate*. In the SERS analysis we have applied here the GNRs were added to the target bacteria suspensions, incubated at room temperature about 30 min, then they were dropped onto the silicon wafers; dried and the surfaces were first observed with the microscope (attached to the Raman Spectrometer) and images were taken. Then we have focused on the selected target bacteria and collected the SERS data. Note that it was possible to focus onto individual bacteria and take the SERS image, indicating that our data is demonstrating almost single bacterial detection.

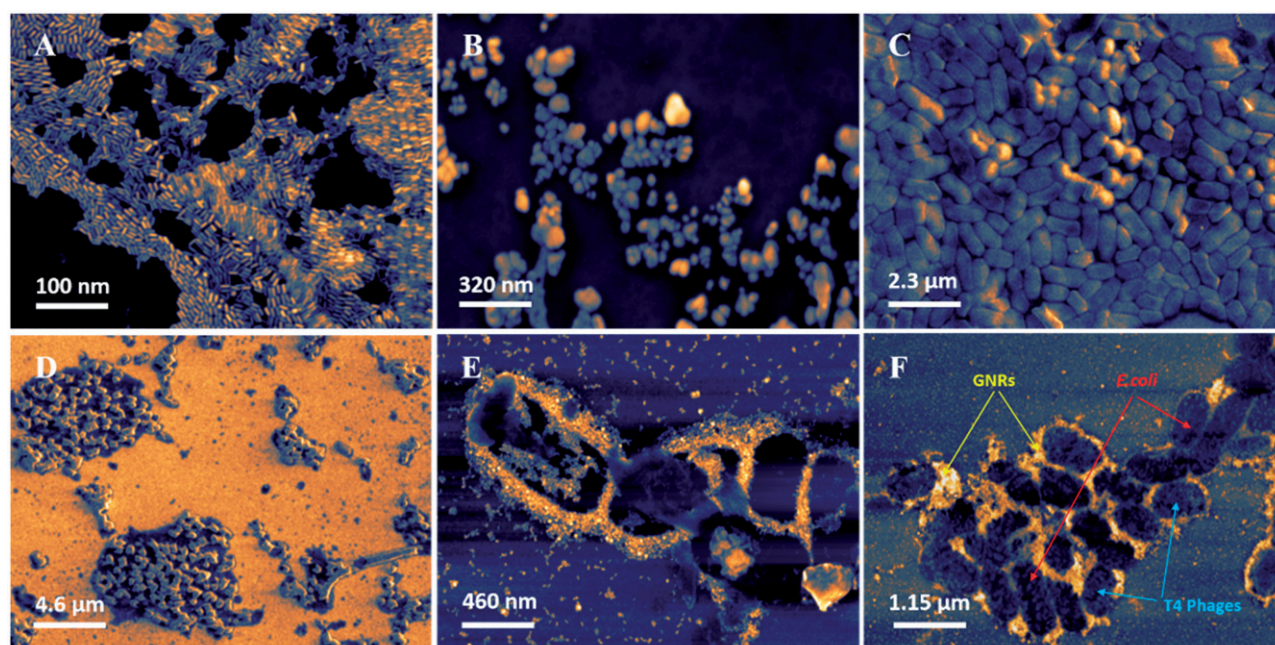


**Figure 2.** Representative SEM images taken on the substrate – silicon wafer surfaces. (A) GNRs; (B) T4 phages; (C) *E. coli* K12; (D) *E. coli* K12 interacted with T4 phages (some of them already); (E) GNRs interacted with *E. coli* K12 in suspensions then dropped on the substrate surface; and (F) three together – *E. coli* + GNRs attached to the bacteria + T4 phages accumulated on the bacteria (at very early stage – no destruction yet). A scanning probe image processing was applied.

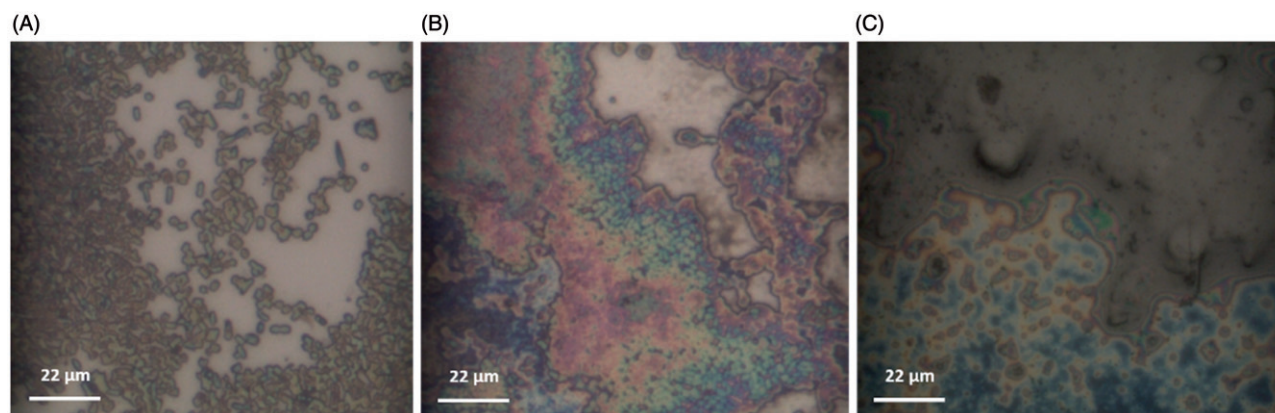


**Figure 3.** Representative images taken with the “transmission and reflection illumination microscope” attached to the Raman spectrometer: (A) *E. coli* K12 on substrate surfaces; (B) GNRs on bacteria (shinning red brown color); and (C) after addition of phages which destroyed almost all bacteria on the surfaces and images “look like lubricated with oil” were observed. A scanning probe image processing was applied.

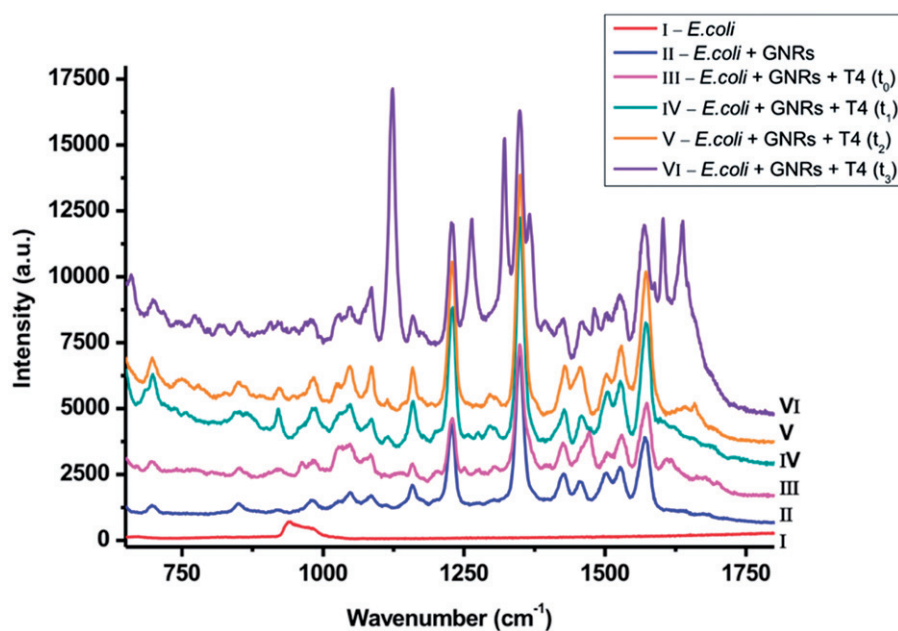


**Figure 4.** Representative SERS spectra: (I) *E. coli* K12 on the substrate (silica) surfaces; (II) *E. coli* K12 first interacted with the GNRs in suspensions then dropped on the substrate surfaces; (III) T4 phages nanoemulsions were dropped on the substrates carrying *E. coli* K12 and GNRs – just after addition ( $t_0$ ); (IV) the same – after 10 min ( $t_1$ ); (V) the same – after 20 min ( $t_2$ ); and (VI) the same after 40 min ( $t_3$ ).

In the following step, T4 phages were placed on the substrates having GNRs accumulated bacteria, and SERS data were collected at selected time intervals. Several data were collected at many different points on the sample, and these experiments were repeated many times. Representative SERS spectra are given in Figure 4. The peaks were quite sharp and intense, note that these were single bacterial cell level therefore “the limits of detection” which was cellular level – may be considered as very notable result of this study. This may be attributed to the localized surface plasmon effects of the GNR aggregates on the bacterial wall as also demonstrated in Figure 2 given/discussed above.

It should be noted that the substrate platform was silicon wafer – which does not give any spectral response between 650 and 1800  $\text{cm}^{-1}$  therefore could not overlap the bacterial/phage peaks. The spectrum of the surfaces carrying only bacteria (no GNRs no bacteriophages) is in the bottom of the figure (the curve I) which is expected because the silica surface

is not a SERS substrate, rather a platform with no plasmonic properties. The curve II is a typical spectrum of *E. coli* carrying GNRs on their surfaces, due to very strong plasmonic effects of the GNRs aggregates on the bacterial wall allowed us to obtain the Raman spectra of the *E. coli* with sharp and clear representative peaks.

In the second step the T4 phage nanoemulsions were dropped onto the silicon wafers evaluated in the previous step – carrying *E. coli* + GNRs and the SERS data were collected at selected time intervals – 10, 20 and 40 min – the representative spectra are illustrated as the curves III, IV, V and VI, respectively. Notice that the first three curves are almost identical – there are changes in the intensities of some peaks but not significant. However, the curve VI was very different than the others. It should be noted that phages did attack their target bacteria, infected and destroyed almost all in about 30–40 min as also demonstrated in Figure 3(C). There were few new/very strong peaks at 1124,



1260, 1320, 1367, 1602 and  $1639\text{ cm}^{-1}$  which do not exist (or very weak) in the *E. coli* spectra (*the curves II*).

It should be noted that Raman spectra for many rather small molecules/biomolecules are very unique. Therefore, it is rather easy to identify these molecules – quite specifically and sensitively – by using those SERS spectra – commonly called “fingerprints”. There are also several studies in the related literature for detection of bacteria including *E. coli* with SERS using silver and gold nanoparticles and nanostructured surfaces for enhancement. Almost all of them based on target identification of the peaks (fingerprints) on the spectra for detection of bacteria – which is the main point/difference of the present study in which we are not targeting identification of those peaks for detection but using specific phages as described above. The rationale of this way of thinking is that there are differences and similarities in the peak positions and also intensities of the SERS spectra obtained for different bacteria – but more importantly there are also significant differences in the *E. coli* spectra published by different groups for *E. coli*. It is quite understandable, bacteria are not a simple molecule/entity, it is a huge pool of different molecules from simple to highly complex 3D structures and molecular weights. Especially biopolymers, like DNA/RNA, proteins, polysaccharides are formed of similar units but with different numbers. Having the same or even similar SERS spectra – even for the same target bacteria is almost impossible – assignments of the characteristic peaks is only an approximation. The differences could also be due to different methods of sample preparation and measurement and possible conformational changes of the cellular biopolymers (proteins, etc.) when they interacted with different platform nanostructured surfaces or nanoparticles. When using nanoparticles as SERS enhancers, it is generally agreed also that colloid reproducibility, particle size and aggregation, and their relative number to the target bacteria within the medium may also influence the magnitude of enhancement and therefore the intensities.

Some of the characteristic peaks can be summarized as follows: It is generally agreed there are some representative similar peaks mostly in the regions  $500\text{--}800\text{ cm}^{-1}$  and  $1100\text{--}1700\text{ cm}^{-1}$  but there are differences mostly in the region  $800\text{--}1000\text{ cm}^{-1}$  [28,29,31,32,50]. The double peak at about  $960\text{ cm}^{-1}$  is due to the C–C stretch (or C–C–N stretch) which is abounding for various proteins in the cell [32,51]. Note also that the peaks in the regions  $600\text{--}900\text{ cm}^{-1}$  and  $1200\text{--}1400\text{ cm}^{-1}$  for *E. coli* are similar to those for Flavin adenine dinucleotide (FAD). The Flavin FAD and Flavin adenine mononucleotide (FMN), which are located in the cell walls of bacteria, are coenzymes that participate in the respiratory processes in a living cell [28,32,52]. The bacterial amide fingerprint located are observed at  $1620\text{--}1640\text{ cm}^{-1}$  in the SERS spectra for *E. coli*, however it may be overlaid with the water peak at  $1635\text{ cm}^{-1}$  [32].

Lan et al. [33] have reported the strict differences for *E. coli* and *S. typhimurium* in the peak position and relative strength. They have pointed out the following peaks and corresponding sources:  $659\text{ cm}^{-1}$  for guanine (C–S);  $722\text{ cm}^{-1}$  for adenine;  $960\text{ cm}^{-1}$  for C=C or tyrosine;  $997\text{ cm}^{-1}$  for phenylalanine or glucose;  $1027\text{ cm}^{-1}$  for a ring stretching, or (C–H)

deformation;  $1086\text{ cm}^{-1}$  for phenylalanine;  $1169\text{ cm}^{-1}$  for 12-methyltetradecanoic acid or 15-methylpalmitic acid or acetoacetate;  $1248\text{ cm}^{-1}$  for C–H<sub>2</sub> stretching;  $1335\text{ cm}^{-1}$  for C–H<sub>2</sub> deformation or tryptophan;  $1472\text{ cm}^{-1}$  C–H<sub>2</sub> deformation of the protein molecules;  $1535\text{ cm}^{-1}$  for adenine, cytosine and guanine;  $1601\text{ cm}^{-1}$  for tyrosine, (C–N) stretching vibration;  $1715\text{ cm}^{-1}$  for C=O.

Naja et al. [36] have reported that peaks at  $600\text{--}800\text{ cm}^{-1}$  and at  $1500\text{--}1700\text{ cm}^{-1}$  could be attributed to nucleic acids and reflected the presence of adenine, guanine, cytosine and thymine (or uracil for RNA) molecules. The peak at  $990\text{ cm}^{-1}$  indicates the presence of phenylalanine molecule as an important aromatic amino-acid residue. The peaks at  $721$  and  $1029\text{ cm}^{-1}$  correspond to the presence of carbohydrate compounds. The peaks at  $1300\text{--}1400\text{ cm}^{-1}$  are generally assigned to protein groups whereas peaks around  $1462\text{ cm}^{-1}$  are attributed to lipids.

The band attribution of the *E. coli* spectrum obtained in this work was based on similar spectra found in the related literature. In detail, the vibrational spectra of *E. coli* exhibited some bands near  $2922\text{ cm}^{-1}$  (not shown) due to the CH<sub>2</sub> asymmetric stretching vibration and the peaks at  $1605\text{--}1690\text{ cm}^{-1}$  are due to the deformation vibration of N–H or the stretching vibration in C–N of the amide I groups. The  $1552\text{ cm}^{-1}$  peak corresponds to different organic vibrations between C, N and H in amide or other groups. The peaks at  $1485$ ,  $1462$ ,  $1355$  and  $1271\text{ cm}^{-1}$  are attributed to the NH<sub>2</sub> stretching in adenine and guanine, to the CH<sub>2</sub> scissoring deformation in lipid groups, to the CH deformation vibrations and to amide III components. In addition, the peaks at  $1056$  and  $1235\text{ cm}^{-1}$  are attributed to the stretching vibration of C–C in alkanes and to the vibration of N–H, respectively. The band attribution in the region of  $500\text{--}800\text{ cm}^{-1}$  are more difficult since the peaks were weaker and less resolved. The observed peaks come from amino-acids, polysaccharides, lipids, and sugars. The  $1008\text{ cm}^{-1}$  band associated with the aromatic ring breathing mode. In brief, the Raman spectrum was reported to consist of several small peaks, occurring between  $500$  and  $1700\text{ cm}^{-1}$ , and two dominant peaks, at  $1355$  and  $1635\text{ cm}^{-1}$ , respectively.

The results of different bacteria like *E. coli* and *S. typhimurium* show the differences in structure and composition of proteins in both species. The peaks at  $1530$  and  $1535\text{ cm}^{-1}$  represent adenine, cytosine and guanine. Amide III band is observed at  $1232\text{ cm}^{-1}$  in the *S. typhimurium* spectrum. The bands at  $722\text{ cm}^{-1}$  and  $729\text{ cm}^{-1}$  are the deformational vibrations of adenine, and these bands are the typical spectral characteristics of DNA in *E. coli* and *S. typhimurium*. There are also different bands which are not interpreted in detail as they are not very conclusive, but they might be affected by cell lysates.

## Conclusions

In this “proof of concept” study, a very simple SERS strategy was applied in which target bacteria (i.e. *E. coli*) were interacted with GNRs in suspensions, and then they were dropped onto plain silica substrate surfaces for detection. As clearly demonstrated in the electron microscope images the

positively loaded GNRs were heavily accumulated around the negatively charged bacterial cell walls which allowed us to collect the SERS spectra (the “fingerprints” of the target bacteria) without using *any SERS platform* – only as a result of enhancing effects of the plasmonic GNRs accumulated onto the bacteria – which was one of the important results of this study. In the second step, bacteriophages (as the specific bioprobes) were dropped onto those surfaces and SERS data were collected by focusing on even individual bacterial cells at different time intervals up to 40 min. Bacteriophages are viruses which *do infect only living bacteria* quite specifically even at serotype level. When they infect their target bacteria, after an about 20–30 min propagation process their number increases about 300 times even larger – that means a very significant increase in the detection signal. In this study, the SERS data collected with time in the tests after addition phages onto the GNRs–bacteria complexes on the silica platforms exhibited that a number of new quite intense/sharp were appeared in about 30–40 min. It should be noted that there was no change in the SERS spectra of the non-target bacteria (i.e. *S. aureus* here) with time after addition of T4 phage which was specific only for the target bacteria (i.e. *E. coli* here). This was the main result of this study – demonstrated that one could detect the target bacteria very specifically and sensitively (even at one bacterial cell level) using bacteriophages as bioprobes and plasmonic nanoparticles (i.e. GNRs here).

## Acknowledgements

This study is partially supported by The KOSGEB project of NanoBMT-Başkent University-TEKMER and EU-FP7-IAPP NanobacterphageSERS and E. Piskin was supported as an *Honorary Member* of Turkish Academy of Sciences. This study was a part of the PhD thesis of Farzaneh Moghtader – contributions of Aysel Tomak, Aytac Gul and Evrim Balçı from İYTE are greatly acknowledged.

## Disclosure statement

No potential conflict of interest was reported by the authors.

## References

- [1] Batz MB, Doyle MP, Morris JG, et al. Attributing illness to food. *Emerging Infect Dis.* 2005;11:993–999.
- [2] Garcia P, Rodriguez L, Rodriguez A, et al. Food biopreservation: promising strategies using bacteriocins, bacteriophages and endolysins. *Trends Food Sci Technol.* 2010;21:373–382.
- [3] Wells JG, Davis BR, Wachsmuth IK, et al. Laboratory investigation of hemorrhagic colitis outbreaks associated with a rare *Escherichia coli* serotype. *J Clin Microbiol.* 1983;18:512–520.
- [4] EFSA. 2009. Available from: [http://www.efsa.europa.eu/EFSA/efsa\\_locale1178620753812\\_121190203\\_1795.htm](http://www.efsa.europa.eu/EFSA/efsa_locale1178620753812_121190203_1795.htm)
- [5] MicroSEQ® *E. coli* O157:H7 Detection Kit, 2014. Available from: <http://tools.lifetechnologies.com/content/sfs/brochures/CO13764.pdf>
- [6] CNN. *E. coli* Outbreaks Fast Facts, 2014. Available from: <http://edition.cnn.com/2013/06/28/health/e-coli-outbreaks-fast-facts>
- [7] Srivastava SK, Hamo HB, Kushmaro A, et al. Highly sensitive and specific detection of *E. coli* by a SERS nanobiosensor chip utilizing metallic nanosculptured thin films. *Analyst.* 2015;140:3201–3209.
- [8] Belgrader P, Bennett W, Hadley D, et al. PCR detection of bacteria in seven minutes. *Science.* 1999;284:449–450.
- [9] Edelstein RL, Tamanaha CR, Sheehan PE, et al. The BARC biosensor applied to the detection of biological warfare agents. *Biosens Bioelectron.* 2000;14:805–813.
- [10] Gau J, Lan EH, Dunn B, et al. A MEMS based amperometric detector for *E. Coli* bacteria using self-assembled monolayers. *Biosens Bioelectron.* 2001;16:745–755.
- [11] Mothershed EA, Whitney AM. Nucleic acid-based methods for the detection of bacterial pathogens: present and future considerations for the clinical laboratory. *Clin Chim Acta.* 2006;363:206–220.
- [12] Byrne B, Stack E, Gilmartin N, et al. Antibody-based sensors: principles, problems and potential for detection of pathogens and associated toxins. *Sensors (Basel).* 2009;9:4407–4445.
- [13] Van Dorst B, Mehta J, Bekaert K, et al. Recent advances in recognition elements of food and environmental biosensors: a review. *Biosens Bioelectron.* 2010;26:1178–1194.
- [14] Farabullini F, Lucarelli F, Palchetti I, et al. Disposable electrochemical genosensor for the simultaneous analysis of different bacterial food contaminants. *Biosens Bioelectron.* 2007;22:1544–1549.
- [15] Balasubramanian S, Sorokulova IB, Vodyanoy VJ, et al. Lytic phage as a specific and selective probe for detection of *Staphylococcus aureus* – a surface plasmon resonance spectroscopic study. *Biosens Bioelectron.* 2007;22:948–955.
- [16] Singh A, Senapati D, Wang S, et al. Gold nanorod based selective identification of *Escherichia Coli* bacteria using two-photon Rayleigh scattering spectroscopy. *ACS Nano.* 2009;3:1906–1912.
- [17] Singh A, Poshtiban S, Evoy S. Recent advances in bacteriophage based biosensors for food-borne pathogen detection. *Sensors (Basel).* 2013;13:1763–1786.
- [18] Lanh LT, Hoa TT, Cuong ND, et al. Shape and size controlled synthesis of Au nanorods: H<sub>2</sub>S gas-sensing characterizations and antibacterial application. *J Alloys Comp.* 2015;635:265–271.
- [19] Li CZ, Male KB, Hrapovic S, et al. Fluorescence properties of gold nanorods and their application for DNA biosensing. *Chem Comm.* 2005;113:3924–3926.
- [20] Pan B, Cui D, Xu P, et al. Study on interaction between gold nanorod and bovine serum albumin. *Coll Surf A.* 2007;295:217–221.
- [21] Huang H, Tang C, Zeng Y, et al. Label-free optical biosensor based on localized surface plasmon resonance of immobilized gold nanorods. *Coll Surf B: Biointerface.* 2009;71:96–101.
- [22] Ma Z, Tian L, Wang T, et al. Optical DNA detection based on gold nanorods aggregation. *Anal Chim Acta.* 2010;673:179–184.
- [23] Won YH, Huh K, Stanciu LA. Au nanospheres and nanorods for enzyme-free electrochemical biosensor applications. *Biosens Bioelectron.* 2011;26:4514–4519.
- [24] Congur G, Sayar F, Erdem A, et al. Voltammetric and impedimetric DNA detection at single-use graphite electrodes modified with gold nanorods. *Coll Surf B Biointerfaces.* 2013;112:61–66.
- [25] Moghtader F, Congur G, Zareie HM, et al. Impedimetric detection of pathogenic bacteria with bacteriophages using gold nanorods deposited graphite electrodes. *RSC Adv.* 2016;6:97832–97839.
- [26] Holt RE, Cotton TM. Surface-enhanced resonance Raman and electrochemical investigation of glucose oxidase catalysis at a silver electrode. *J Am Chem Soc.* 1989;111:2815–2821.
- [27] Efrima S, Bronk BV. Silver colloids impregnating or coating bacteria. *J Phys Chem B.* 1998;102:5947–5950.
- [28] Zeiri L, Bronk BV, Shabtai Y, et al. Surface-enhanced Raman Spectroscopy as a tool for probing specific biochemical components in bacteria. *Appl Spectrosc.* 2004;58:33–40.
- [29] Jarvis RM, Goodacre R. Discrimination of bacteria using surface-enhanced Raman spectroscopy. *Anal Chem.* 2004;76:565–579.
- [30] Jarvis RM, Brooker A, Goodacre R. Surface-enhanced Raman spectroscopy for bacterial discrimination utilizing a scanning electron microscope with a Raman spectroscopy interface. *Anal Chem.* 2004;76:5198–5202.



- [31] Sengupta A, Laucks ML, Dildine N, et al. Bioaerosol characterization by surface-enhanced Raman spectroscopy (SERS). *J Aerosol Sci.* 2005;36:651–664.
- [32] Sengupta A, Mujacic M, Davis E. Detection of bacteria by surface-enhanced Raman spectroscopy. *Anal Bioanal Chem.* 2006;386:1379–1386.
- [33] Lan S, Zhang P, Zheng D, et al. Rapid detection of *Escherichia coli* and *Salmonella typhimurium* by surface-enhanced Raman scattering. *Optoelectron Lett.* 2015;11:157–160.
- [34] Patel IS, Premasiri WR, Moir DT, et al. Barcoding bacterial cells: a SERS based methodology for pathogen identification. *J Raman Spectrosc.* 2008;39:1660–1672.
- [35] Chen J, Wu X, Huang Y, et al. Chemical detection of *E. coli* using SERS active filters with silver nanorod array. *Sen Actua: B Chem.* 2014;191:485–490.
- [36] Naja G, Bouvrette P, Hrapovic S, et al. Raman-based detection of bacteria using silver nanoparticles conjugated with antibodies. *Analyst.* 2007;132:679–686.
- [37] Grow AE, Wood LL, Claycomb JL, et al. New biochip technology for label-free detection of pathogens and their toxins. *J Microbiol Methods.* 2003;53:221–227.
- [38] Montoya JR, Armstrong RL, Smith GB. Detection of *Salmonella* using surfaced enhanced Raman scattering. *Proc SPIE.* 2003; 5085:144–152.
- [39] Laucks ML, Sengupta A, Junge K, et al. Comparison of psychroactive arctic marine bacteria and common mesophilic bacteria using surface-enhanced Raman spectroscopy. *Appl Spectrosc.* 2005;59:1222–1228.
- [40] Zeiri L, Efrima S. Surface-enhanced Raman spectroscopy of bacteria: the effect of excitation wavelength and chemical modification of the colloidal milieu. *J Raman Spectrosc.* 2005;36:667–675.
- [41] Guven B, Basaran-Akgul N, Temur E, et al. SERS-based sandwich immunoassay using antibody coated magnetic nanoparticles for *Escherichia coli* enumeration. *Analyst.* 2011;136:740–748.
- [42] Tamer U, Cetin D, Suludere Z, et al. Gold-coated iron composite nanospheres argeted the detection of *Escherichia coli*. *Int J Mol Sci.* 2013;14:6223–6240.
- [43] Sambrook J, Russell DW. *Molecular cloning: a laboratory manual.* New York (NY): Cold spring Harbour Laboratory Press; 1989.
- [44] Mejri MB, Baccar H, Baldrich E, et al. Impedance biosensing using phages for bacteria detection: generation of dual signals as the clue for in-chip assay confirmation. *Biosens Bioelectron.* 2010;26:1261–1267.
- [45] Moghtader F, Egri S, Piskin E. Phages in modified alginate beads. *Artif Cells Nanomed Biotechnol.* 2017;45:357–363.
- [46] Nikoobakht B, El-Sayed MA. Preparation and growth mechanism of gold nanorods (NRs) using seed-mediated growth method. *Chem Mater.* 2003;15:1957–1962.
- [47] Gole AA, Murphy CJ. Seed-mediated synthesis of gold nanorods: role of the size and nature of the seed. *Chem Mater.* 2004;16:3633–3640.
- [48] Turk M, Tamer U, Alver E, et al. Fabrication and characterization of gold-nanoparticles/chitosan film: a scaffold for L929-fibroblasts. *Artif Cells Nanomed Biotechnol.* 2013;41:395–401.
- [49] Tomak A, Zareie HM. Gold nanorod encapsulated bubbles. *RSC Adv.* 2015;5:38842–38845.
- [50] Sengupta A, Laucks ML, Davis E. Surface-enhanced Raman spectroscopy of bacteria and pollen. *Appl Spectrosc.* 2005;59: 1016–1023.
- [51] Spiro TG, Gaber BP. Laser Raman scattering as a probe of protein structure. *Annu Rev Biochem.* 1977;46:553–570.
- [52] Morii MC, Beinstock RJ. 1986. *Spectroscopy of biological systems.* New York (NY): Wiley.

Copyright of Artificial Cells, Nanomedicine & Biotechnology is the property of Taylor & Francis Ltd and its content may not be copied or emailed to multiple sites or posted to a listserv without the copyright holder's express written permission. However, users may print, download, or email articles for individual use.